INTERNATIONAL JOURNAL OF STRUCTURAL CHANGES IN SOLIDS – Mechanics and Applications
Volume 4, 2012, pp.1-11

IJSCS

A numerical study on effect of strain rate and temperature in the Taylor rod impact problem

Sachin S. Gautam[a], Ravindra K. Saxena*[b]

Abstract

Study of impact problems has important applications in the branch of engineering. In impact problems, the primary design objective is to ensure that the engineering structures do not fail catastrophically when subjected to short duration impact loads. Due to impact, high magnitude of stress waves travel inside the continuum. Material experiences large plastic strain and high temperature rise on the impacting face. A three-dimensional, large deformation, thermo-elasto-plastic, dynamic, contact, finite element formulation is developed to study the effect of strain rate and temperature on the deformation and stress fields in the Taylor rod impact problem. It is found that the equivalent plastic strain gets over-predicted to a significant extent if the effect of the strain rate is not included in the formulation.

Keywords: High velocity impact; Thermo-elasto-plastic formulation; Numerical algorithms; Taylor rod impact Test; Finite element method.

1. Introduction

Impact phenomena occur in many engineering situations. The basic characteristics of an impact phenomenon are very short duration, high force levels, large plastic deformations and strain rates and rise in temperature. Rigorous analysis of an impact problem requires the consideration of all these aspects. When a material is plastically deformed, most of the energy is converted into heat. This leads to thermal gradients that soften the material differentially creating high local strain rates. This, in turn, induces additional temperature rise because of the correlation between strain rates and temperature rise. This thermo-mechanical phenomenon becomes more severe in high velocity impacts.

A commonly employed procedure in analyzing thermo-elasto-plastic problem is to decouple it by solving it in two steps in each increment: the dynamic, elasto-plastic deformation analysis at known temperature field followed by the transient heat transfer analysis at the fixed configuration [Wrigger and Miehe 1994; Xing and Makinouchi 2002]. The constitutive equation for thermo-elasto-plastic behavior differs from that of the elasto-plastic behavior in two respects. First, the incremental strain consists of three parts: (i) elastic, (ii) plastic and (iii) thermal. Secondly, the plastic potential for thermo-elasto-plastic behavior also depends on the temperature and strain rates. Thus, the corresponding incremental stress-strain relation includes an additional term consisting of temperature and strain rate effects besides the usual term containing the fourth-order elasto-plastic constitutive tensor. Additionally, this tensor gets multiplied by the difference between the total and thermal strain. In dynamic thermo-elasto-plastic problems, the incremental temperature is determined by solving the unsteady heat conduction equation where the heat source term consists of the incremental plastic work done per unit volume.

In plastic deformation problems, a large fraction of the mechanical work is converted into heat. Mason *et al.* (1993) made the first attempt to measure this fraction using dynamic experiments performed over a wide range of strains and strain rates. They demonstrated that the fraction of plastic work getting converted into heat depends substantially on the strain and strain rate levels.

Taylor (1948) determined the dynamic yield stress of one dimensional specimen through the impact of cylindrical specimen on a flat rigid target. This problem, generally known as the Taylor rod impact problem or test, is used as an experimental and numerical test for determining the mechanical behavior of materials subjected to high strain rates. Several authors have studied the Taylor rod impact problem experimentally,

[a]AICES, RWTH Aachen University, Aachen, 52062, Germany
[b]Sant Longowal Institute of Engineering and Technology, Sangrur, Punjab, INDIA,
Email: rksaxena04@yahoo.com

theoretically and numerically. Only some latest references which incorporate the dependence of the yield stress on the strain rate and temperature are discussed in the present work. Celentano (2002) did a numerical simulation of Taylor rod impact test using in-house finite element code. Johnson-Cook model (1985) was used to describe the dependence of the yield stress on the strain, strain rate and temperature. Few experiments were also performed to validate the numerical code. Brünig and Driemeier (2007) performed the numerical simulation of symmetrical Taylor rod impact test (i.e., the impact of two identical cylindrical rods) using the LS-DYNA Explicit finite element code. They proposed a functional for determining the dependence of strain, strain rate and temperature. The constants were determined from experimental work available in literature. Teng *et al.* (2005) investigated the fracture phenomena and mechanisms in Taylor rod impact test using explicit ABAQUS finite element code. They employed a recently developed ductile fracture locus with the cut-off value for the negative stress triaxiality (ratio of hydrostatic stress and equivalent stress) as '(-1/3)'. Johnson-Cook model (1985) was used to describe the dependence of the yield stress on the strain, strain rate and temperature. Even though all these researchers have accounted for the dependence of the yield stress on the strain rate and temperature, the effects of these two parameters (i.e., the strain rate and temperature) on the deformation and stress fields have not been explicitly investigated.

It is observed from the literature that the dependence of the yield stress on the strain rate and temperature on the deformation and stress fields have not been explicitly investigated. The objective of the present work is to bring out the effect of strain rate and temperature on the deformation behavior and stress distribution in high velocity impact problems. Specifically, the effect of these quantities is studied on two continuum parameters which influence the fracture (Saxena and Dixit 2011), the equivalent plastic strain and triaxiality.

A three dimensional, large deformation, thermo-elasto-plastic, dynamic, contact, finite element- finite difference formulation is developed for this purpose. Elastic behaviour is modeled by the generalized Hooke's law and the plastic behavior is modeled by an associated flow rule based on the von-Mises yield function. The variable yield stress is assumed to depend on equivalent plastic strain, equivalent plastic strain rate and temperature by Johnson-Cook model (1985). Incremental logarithmic strain measure is used. The incremental stress is made objective by evaluating it in a frame rotating with the material particle. The radial backward return algorithm is used to correct the updated stress iteratively so that it lies on the yield surface. Updated Lagrangian formulation (Bathe 1996) is used to develop the incremental finite element equations. A finite difference scheme is used for carrying out the discretization in time. Newmark's algorithm, which is found to be suitable in terms of stability and accuracy among the various finite difference schemes, is used for this purpose. Modified Newton-Raphson iterative method is used for solving these nonlinear incremental equations. Contact iterations are carried out to find the contact reactions (Zhong 1993) in each of the Newton-Raphson iteration. The incremental analysis is decoupled by performing it in two steps. In the first step, the dynamic thermo-elasto-plastic analysis is carried out at a known temperature. In the second step, the transient heat transfer analysis is carried out at fixed configuration by using the incremental plastic work per unit volume as the heat source. The Galerkin's finite element method and a finite difference scheme are used to convert the unsteady non-linear heat conduction equation into a set of algebraic equations.

2. Dynamic Thermo-Elasto-Plastic Formulation

2.1 *Incremental strain-displacement relation*

The incremental logarithmic strain measure, used in the present formulation, is defined by (Bathe 1996)

$$ {}_t d\varepsilon_{ij}^{L} = \ln({}^t\ell_i)\delta_{ij} \qquad \text{(no sum over } i\text{)} \tag{1} $$

where δ_{ij} is the Kronecker's delta and ${}^t\ell_i$ are the principal values of the incremental right stretch tensor ${}^tU_{ij}$.

2.2 *Thermo-elasto-plastic constitutive equation*

During the plastic deformation, the plastic work is transformed into heat. This phenomenon raises the temperature of the body. This temperature rise induces a thermal strain inside the body. The incremental logarithmic strain ${}_t d\varepsilon_{ij}^{L}$ can therefore be considered as the sum of three parts: the incremental elastic strain ${}_t d\varepsilon_{ij}^{eL}$, the incremental plastic strain ${}_t d\varepsilon_{ij}^{pL}$ and the incremental thermal strain ${}_t d\varepsilon_{ij}^{TL}$:

$$ {}_t d\varepsilon_{ij}^{L} = {}_t d\varepsilon_{ij}^{eL} + {}_t d\varepsilon_{ij}^{pL} + {}_t d\varepsilon_{ij}^{TL} \tag{2} $$

Then, the incremental elastic stress-strain relationship can be expressed as follows:

$$ {}_t d\sigma_{ij} = \mathrm{C}^{E}_{\mathrm{i\,jkl}} \left({}_t d\varepsilon^{L}_{kl} - {}_t d\varepsilon^{pL}_{kl} - {}_t d\varepsilon^{TL}_{kl} \right) \tag{3} $$

Here, ${}_t d\sigma_{ij}$ is the incremental stress tensor and $\mathrm{C}^{E}_{\mathrm{i\,jkl}} = \lambda\delta_{ij}\delta_{kl} + 2\mu\delta_{ik}\delta_{jl}$ is the elastic constitutive tensor where λ and μ are the Lame's constants.

It is assumed that the strain rate tensor (i.e., the symmetric part of the velocity gradient tensor), denoted by ${}^t\dot{\varepsilon}^{L}_{ij}$ can be additively decomposed into the elastic and plastic parts. Thus

$$ {}^t\dot{\varepsilon}^{L}_{ij} = {}^t\dot{\varepsilon}^{eL}_{ij} + {}^t\dot{\varepsilon}^{pL}_{ij} \tag{4} $$

where ${}^t\dot{\varepsilon}^{eL}_{ij}$ and ${}^t\dot{\varepsilon}^{pL}_{ij}$ are the elastic and plastic parts respectively of ${}^t\dot{\varepsilon}^{L}_{ij}$. Equivalent plastic strain rate (an invariant of ${}^t\dot{\varepsilon}^{pL}_{ij}$) is defined as

$$ {}^t\dot{\varepsilon}^{pL}_{eq} = \sqrt{\frac{2}{3}\, {}^t\dot{\varepsilon}^{pL}_{ij}\, {}^t\dot{\varepsilon}^{pL}_{ij}} \tag{5} $$

The relation between ${}^t\dot{\varepsilon}^{pL}_{eq}$ and ${}^t\varepsilon^{pL}_{eq}$, for small increment, is given by

$$ {}^t\dot{\varepsilon}^{pL}_{eq} = \int {}^t\dot{\varepsilon}^{pL}_{eq}\, dt = \int {}_t d\varepsilon^{pL}_{eq}, \qquad {}_t d\varepsilon^{pL}_{eq} = \sqrt{\frac{2}{3}\, {}_t d\varepsilon^{pL}_{ij}\, {}_t\varepsilon^{pL}_{ij}} \tag{6} $$

where dt is the incremental time.

For a material yielding according to the von-Mises criterion with isotropic hardening (due to strain and strain rate) and isotropic temperature softening, the yield function is given by (Bathe 1996)

$$ {}^t f(\sigma_{ij}) = {}^t\sigma_{eq}(\sigma_{ij}) - {}^t\sigma_Y\left({}^t\varepsilon^{pL}_{eq}, {}^t\dot{\varepsilon}^{pL}_{eq}, T \right), \tag{7} $$

where ${}^t\sigma_Y$ is the variable yield stress of the material. The equivalent stress ${}^t\sigma_{eq}$ is defined as

$$ {}^t\sigma_{eq} = \sqrt{\frac{3}{2}\, {}^t\sigma'_{ij}\, {}^t\sigma'_{ij}} \tag{8} $$

Here, ${}^t\sigma'_{ij}$ is the deviatoric part of ${}^t\sigma_{ij}$. The dependence of ${}^t\sigma_Y$ on ${}^t\varepsilon^{pL}_{eq}$, ${}^t\dot{\varepsilon}^{pL}_{eq}$ and ${}^t T$ is governed by the Johnson-Cook model (1985):

$$ \begin{aligned} {}^t\sigma_Y &= H\left({}^t\varepsilon^{pL}_{eq}, {}^t\dot{\varepsilon}^{pL}_{eq}, T \right) \\ &= A^p \left(\varepsilon^{pL}_{ref} + {}^t\varepsilon^{pL}_{eq} \right)^n \left(1 - \left(\frac{{}^tT - T_{ref}}{T_m - T_{ref}} \right)^{m^p} \right) \left(1 + B^p \ln\left(\frac{{}^t\dot{\varepsilon}^{pL}_{eq}}{{}^t\dot{\varepsilon}^{pL}_{ref}} \right) \right) \end{aligned} \tag{9} $$

where A^p, n, m^p and B^p are the Johnson-Cook parameters, ε^{pL}_{ref} and $\dot{\varepsilon}^{pL}_{ref}$ are the reference strain and strain rate and T_m and T_{ref} are the melting point and reference temperatures respectively.

The incremental plastic strain ${}_t\varepsilon^{pL}_{ij}$ is obtained by the associated flow rule:

$$ {}_t d\varepsilon^{pL}_{ij} = d\lambda \frac{\partial\, {}^t f}{\partial \sigma_{ij}} \tag{10} $$

where $d\lambda$ is a positive scalar. From Eqs. (6) and (8) one can get $d\lambda = {}_t d\varepsilon^{pL}_{eq}$. Setting the total differential of the yield function to zero:

$$ {}_t df \equiv \frac{\partial\, {}^t f}{\partial \sigma_{ij}}\, {}_t d\sigma_{ij} + \frac{\partial\, {}^t f}{\partial\, {}^t\varepsilon^{pL}_{eq}}\, {}_t d\varepsilon^{pL}_{eq} + \frac{\partial\, {}^t f}{\partial\, {}^tT}\, {}_t dT + \frac{\partial\, {}^t f}{\partial\, {}^t\dot{\varepsilon}^{pL}_{eq}}\, {}_t d\dot{\varepsilon}^{pL}_{eq} = 0 \tag{11} $$

This is called the consistency condition. Substituting Eqs. (3) and (10), identifying ${}_t d\varepsilon^{pL}_{eq}$ as $d\lambda$, $\partial\, {}^t\sigma_Y \big/ \partial\, {}^t\varepsilon^{pL}_{eq}$ as ${}^tH'$ in the above equation and solving for $d\lambda$ gives (Hsu 1986)

$$ d\lambda = \frac{\dfrac{\partial\, {}^t f}{\partial \sigma_{ij}}\, {}^t\mathrm{C}^{EP}_{\mathrm{i\,jkl}} \left({}_t d\varepsilon^{L}_{kl} - {}_t d\varepsilon^{TL}_{kl} \right) - \left(\dfrac{\partial\, {}^t f}{\partial\, {}^tT}\, {}_t dT + \dfrac{\partial\, {}^t f}{\partial\, {}^t\dot{\varepsilon}^{pL}_{eq}}\, {}_t d\dot{\varepsilon}^{pL}_{eq} \right)}{\left(\dfrac{\partial\, {}^t f}{\partial\, {}^t\sigma_{rs}}\, {}^t\mathrm{C}^{E}_{rsuv} \dfrac{\partial\, {}^t f}{\partial\, {}^t\sigma_{uv}} + {}^tH' \right)} \tag{12} $$

Substituting the associated flow rule (Eq. 10) and the above expression for $d\lambda$ (Eq. 12), the incremental stress-strain relationship (Eq. 3) becomes

$$ {}_t d\sigma_{ij} = {}^t\mathrm{C}^{EP}_{\mathrm{i\,jkl}}\left({}_t d\varepsilon^{L}_{kl} - {}_t d\varepsilon^{TL}_{kl}\right) + {}^t\mathrm{R}_{ij} \tag{13} $$

where ${}^t\mathrm{R}_{ij}$ and the fourth order elasto-plastic constitutive tensor ${}^t\mathrm{C}^{EP}_{\mathrm{i\,jkl}}$ are given by (Hsu 1986)

$$ \begin{aligned} {}^t\mathrm{C}^{EP}_{\mathrm{i\,jkl}} &= \left(\mathrm{C}^{E}_{\mathrm{i\,jkl}} - \frac{\mathrm{C}^{E}_{\mathrm{i\,jmn}} \dfrac{\partial^t f}{\partial^t \sigma_{mn}} \dfrac{\partial^t f}{\partial^t \sigma_{pq}} \mathrm{C}^{E}_{\mathrm{pqkl}}}{\left(\dfrac{\partial^t f}{\partial^t \sigma_{rs}} \mathrm{C}^{E}_{rsuv} \dfrac{\partial^t f}{\partial^t \sigma_{uv}} + {}^t H' \right)} \right) \\ {}^t\mathrm{R}_{ij} &= \left(\frac{\mathrm{C}^{E}_{\mathrm{i\,jkl}} \dfrac{\partial^t f}{\partial^t \sigma_{kl}} \left(\dfrac{\partial^t \sigma_Y}{\partial^t \dot{\varepsilon}^{pL}_{eq}} {}_t d\dot{\varepsilon}^{pL}_{eq} + \dfrac{\partial^t \sigma_Y}{\partial^t T} {}^t dT \right)}{\left(\dfrac{\partial^t f}{\partial^t \sigma_{rs}} {}^t\mathrm{C}^{E}_{rsuv} \dfrac{\partial^t f}{\partial^t \sigma_{uv}} + {}^t H' \right)} \right) \end{aligned} \tag{14} $$

The incremental stress ${}_t d\sigma_{ij}$ on the left side of Eq. (13) must be an objective stress tensor, i.e., a tensor invariant under the incremental rotation. To make it objective, it is evaluated in the material frame and ${}_t d\sigma_{ij}$ is updated taking into account the material rotation (Varadhan 1997).

2.3 *Integral form of equilibrium equation*

Integral form of the equilibrium equation at time $t+\Delta t$ is given by the virtual work expression (Bathe 1996)

$$ \int_{t+\Delta t_V} {}^{t+\Delta t}\rho\, {}^{t+\Delta t}\ddot{u}_i \delta\left({}_t du_i\right) d\,{}^{t+\Delta t}V + \int_{t+\Delta t_V} {}^{t+\Delta t}\sigma_{ij} \delta\left({}_t d\varepsilon_{ij}\right) d\,{}^{t+\Delta t}V = {}^{t+\Delta t}F \tag{15} $$

where, ${}^{t+\Delta t}\rho$ is the density of the material, ${}^{t+\Delta t}\ddot{u}_i$ is the acceleration vector, ${}_t du_i$ is virtual incremental displacement vector, ${}^{t+\Delta t}\sigma_{ij}$ is Cauchy stress tensor, ${}_t d\varepsilon_{ij}$ is virtual incremental linear strain tensor, ${}^{t+\Delta t}F$ is the virtual work of the specified traction, contact traction and body force and ${}^{t+\Delta t}V$ is the volume of the continuum. Since, the configuration at time $t+\Delta t$ is unknown, this expression is transformed to an integral over the known domain at time t (i.e. ${}^tV$) involving the second Piola-Kirchoff stress tensor ${}^{t+\Delta t}_{\ \ t}P_{ij}$ and the virtual incremental Green Lagrange strain tensor $\delta\left({}_t de_{ij}\right)$ (Bathe 1996). This virtual work expression is further simplified by decomposing ${}^{t+\Delta t}_{\ \ t}P_{ij}$ as the sum of ${}^t\sigma_{ij}$ and ${}_t dP_{ij}$. Decomposing $\delta\left({}_t de_{ij}\right)$ into the linear and non-linear parts, assuming ${}_t dP_{ij}$ and ${}_t d\varepsilon_{kl}$ (i.e., the incremental linear strain tensor) satisfy the constitutive relationship (Eq. 13) and neglecting the higher order terms, Eq. (15) can be written as:

$$ \begin{aligned} &\int_{t_V} {}^t\rho\, {}^{t+\Delta t}\ddot{u}_i \delta\left({}_t du_i\right) d\,{}^tV + \int_{t_V} {}^t\mathrm{C}^{EP}_{\mathrm{i\,jkl}}\left({}_t d\varepsilon_{kl} - {}_t d\varepsilon^{T}_{kl}\right) \delta\left({}_t d\varepsilon_{ij}\right) d\,{}^tV + \int_{t_V} {}^t\mathrm{R}_{ij} \delta\left({}_t d\varepsilon_{ij}\right) d\,{}^tV \\ &+ \int_{t_V} {}^t\mathrm{R}_{ij} \delta\left({}_t d\eta_{ij}\right) d\,{}^tV + \int_{t_V} {}^t\sigma_{ij} \delta\left({}_t d\eta_{ij}\right) d\,{}^tV + \int_{t_V} {}^t\sigma_{ij} \delta\left({}_t d\varepsilon_{ij}\right) d\,{}^tV = {}^{t+\Delta t}F \end{aligned} \tag{16} $$

where the linear and nonlinear parts of the incremental Green-Lagrange strain tensor ${}_t de_{ij}$ are given by

$$ {}_t d\varepsilon_{ij} = \frac{\left({}_t du_{i,j} + {}_t du_{j,i}\right)}{2}, \quad {}_t d\eta_{ij} = \frac{{}_t du_{k,i}\, du_{k,j}}{2}. \tag{17} $$

3. Finite Element-Finite Difference Formulation

The domain is discretized into a number of eight-noded hexahedral elements and the incremental displacement field is approximated over each element by trilinear shape functions (Bathe 1996). Using the finite element approximation, Eq. (16) is converted into a system of second order ordinary differential equations (Bathe 1996)

$$ {}^t[M]\,{}^{t+\Delta t}\{\ddot{U}\} + {}^t[K]_t\{\Delta U\} + {}^t\{f\} = {}^{t+\Delta t}\{F\} + {}^t\{F^T\} - {}^t\{F^M\} \tag{18} $$

where ${}^{t}[M]$ is the global mass matrix, ${}^{t}[K]$ is the global stiffness matrix, ${}^{t}\{f\}$ is the global internal force vector, ${}^{t+\Delta t}\{F\}$ is the global external force vector at $t+\Delta t$, ${}^{t}\{F^{T}\}$ is the global external force vector due to thermal strain and ${}^{t}\{F^{M}\}$ is the global external force vector due to the change in plastic properties. Further, ${}_{t}\{\Delta U\}$ is the global incremental displacement vector and ${}^{t+\Delta t}\{\ddot{U}\}$ is the global acceleration vector at $t+\Delta t$.

To convert Eq. (18) into a system of algebraic equations, the *Newmark's implicit finite difference scheme* (Bathe 1996) is used. After some algebraic manipulations, Eq. (18) reduces to

$$ {}^{t}[K_d]\,{}_{t}\{\Delta U\} = {}_{t}\{\Delta F_d\} \tag{19}$$

where the effective stiffness matrix ${}^{t}[K_d]$ and the effective incremental force vector ${}_{t}\{\Delta F_d\}$ are given by

$$ {}^{t}[K_d] = a_0\,{}^{t}[M] + {}^{t}[K] \tag{20}$$

$$ {}_{t}\{\Delta F_d\} = {}^{t+\Delta t}\{F\} - {}^{t}\{f\} + {}^{t}[M]\left(a_1\,{}^{t}\{\dot{U}\} + a_2\,{}^{t}\{\ddot{U}\}\right) + {}^{t}\{F^{T}\} - {}^{t}\{F^{M}\} \tag{21}$$

where a_0, a_1 and a_2 are the Newmark's parameters (Bathe 1996) and ${}^{t}\{\dot{U}\}$ is the global velocity vector.

The solution of Eq. (19) represents only an approximate solution to the governing equations, because of the linearization and approximation involved in arriving at expression (16). To minimize the error of the approximating solution, the modified Newton-Raphson algorithm (Bathe 1996) is used. The stresses are integrated using the radial backward return algorithm (Bathe 1996). The relationship is modified to include the effect of temperature and strain rate to ensure that the updated state of stress lies on the yield surface.

4. Thermal Formulation

4.1. *Governing equation*

For an isotropic material, three dimensional heat transfer equation in Cartesian coordinates can be expressed as

$$ \left(k\,{}^{t}T_{,i}\right)_{,i} + {}^{t}\dot{q} - \rho c\,{}^{t}\dot{T} = 0 \tag{22}$$

where k is the material conductivity, c is the material specific heat and $\dot{q}$ is the rate of heat generation. It is assumed that the conductivity k, density ρ and specific heat c do not depend on temperature.

4.2. *Heat generation due to plastic work*

Heat generation per unit volume per unit time at a point in the body due to the plastic deformation within time interval Δt is given by

$$ {}^{t}\dot{q}_p = \frac{\beta}{\Delta t}\int_{t}^{t+\Delta t} {}_{t}d\sigma_{ij}\,{}_{t}d\varepsilon_{ij}^{pL} \tag{23}$$

where β is the fraction of plastic work converted to heat. The value of β is found to depend on the strain levels [Taylor and Quinney 1934; Kamlah and Haupt 1997; Hodowany et al. 2000; Mollica et al. 2001]. This fraction increases at the initial levels of plastic deformation and then decreases. Kamlah and Haupt [1997] have pointed out that for "pragmatic view point" the constant value of β is acceptable as a compromise between simplicity and sophistication for engineering applications. The value of β lies in the range of $0.85 \le \beta \le 0.95$ [Farren and Taylor 1925; Gao and Wagoner 1987]. The value of β is taken as 0.9 in the present work.

5. Finite Element-Finite Difference Formulation

The temperature field over the eight-noded hexahedral element is approximated by the tri-linear shape functions (Bathe 1996). Using the finite element approximation, Eq. (22) is converted into a system of first order ordinary differential equations (Bathe 1996).

$$ [C]\,{}^{t}\{\dot{T}\} + [K]\,{}^{t}\{T\} = {}^{t}\{Q\} \tag{24}$$

where ${}^{t}\{T\}$ is the global temperature vector, ${}^{t}\{\dot{T}\}$ is the derivative of ${}^{t}\{T\}$ with respect to time t, $[C]$ is the global specific heat matrix, $[K]$ is the global conductivity matrix and $\{Q\}$ is the global heat flux vector. Using the direct integration method, the system of first order ordinary differential equations is converted into a system of algebraic equations as

$$[A]^{t+\Delta t}\{T\} = {}^{t+\Delta t}_{t}\{B\} \tag{25}$$

where,

$$[A] = ([C] + \alpha\Delta t[K]) \tag{26}$$

$${}^{t+\Delta t}_{t}\{B\} = ([C] - (1-\alpha)\Delta t[K])^{t}\{T\} + \alpha\Delta t\,{}^{t+\Delta t}\{Q\} + (1-\alpha)\Delta t\,{}^{t}\{Q\} \tag{27}$$

Here, α is the parameter of the finite difference scheme (Bathe 1996). Equation (25), which is a set of linear algebraic equations, is solved by the Gauss elimination method.

6. Contact Formulation

The dynamic, large deformation, thermo-elasto-plastic, updated Lagrangian finite element formulation is used for contact analysis with appropriate modifications. The equations, which consist of the kinematic constraints (impenetrability conditions) and the contact force expressions based on the discretization of the contact boundary, are developed using the *Lagrange multiplier method* (Zhong 1993). According to the above formulation it is convenient to choose one contact surface as slave (hitting) and the other as master (target) surface. A node-to-surface contact model is employed for contact analysis in large deformation problem (Zhong 1993).

7. Results and Discussion

An in-house three-dimensional, finite element - finite difference code is developed based on the formulation of Sections 2-6. First, the code is validated by comparing the predicted deformation and temperature in Taylor rod impact problem with experimental and numerical results of Celentano (2002). Next, the effects of strain rate and temperature on equivalent plastic strain and triaxiality in Taylor rod impact problem are studied.

Table 1: Material properties of SAE 1020 steel (Celentano 2002)

Young modulus	E	210 GPa
Poisson ratio	ν	0.3
Density	ρ	7800 kg/m^3
Initial yield stress	${}^{o}\sigma_Y$	333 MPa
Hardening coefficient	A^p	731.7 MPa
Reference strain	ε^{PL}_{ref}	0.01475
Hardening exponent	n	0.1867
Thermal exponent	m^p	1.0
Melting temperature	T_m	$1525\,^0C$
Rate hardening coefficient	B^p	0.05
Reference strain rate	$\dot{\varepsilon}^{PL}_{ref}$	1.0
Thermal conductivity	k	$52\ W/m\,^0C$
Specific heat	c	$450\ J/Kg\,^0C$
Coefficient of thermal expansion	α	$10^{-5}\,^0C^{-1}$

7.1. *Validation*

A coupled thermo-mechanical simulation of Taylor rod impact problem is carried out by considering the impact of a flat-ended cylindrical rod against a rigid wall. The geometric details of the problem are shown in Fig. 1. The rod material is SAE 1020 steel. The material properties are given in Table 1 (Celentano 2002). The heat transfer to the surrounding environment during a short impact span is assumed negligible, thereby adiabatic conditions are considered at the rod boundaries. The reference temperature of the rod is taken as 25 ^0C . Due to

symmetry, only one fourth of the rod is considered for analysis. The finite element mesh consists of 3000 elements and 3731 nodes. The incremental time step is selected as 0.05 μs.

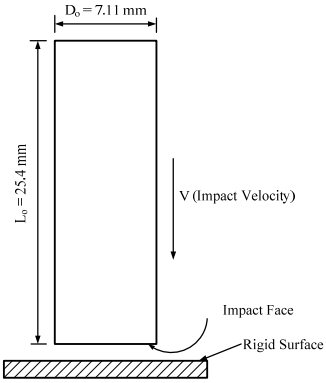

Figure 1: A flat ended cylindrical rod impacting against a rigid surface

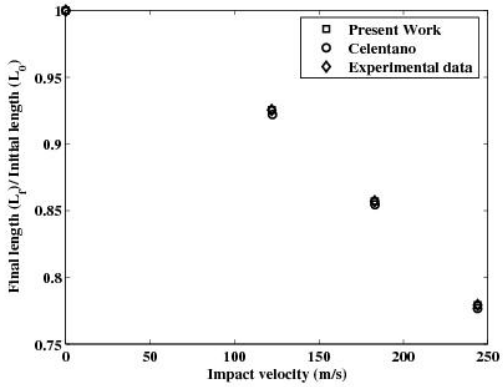

(a) Ratio L_f/L_0

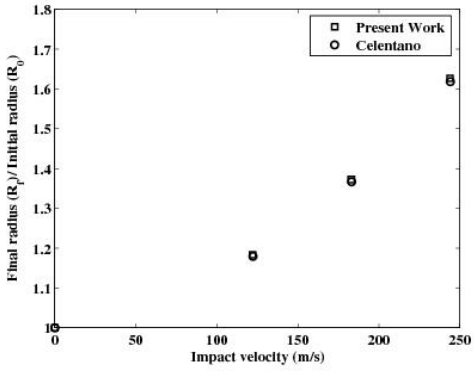

(b) Ratio R_f/R_0

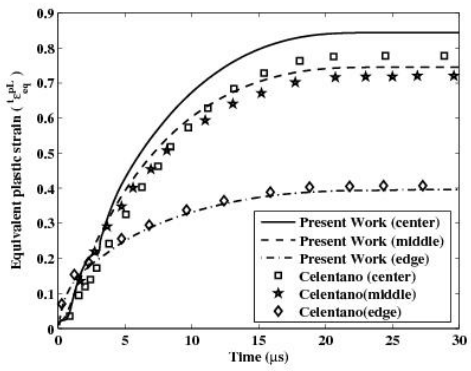

(c) Equivalent plastic strain on impact face

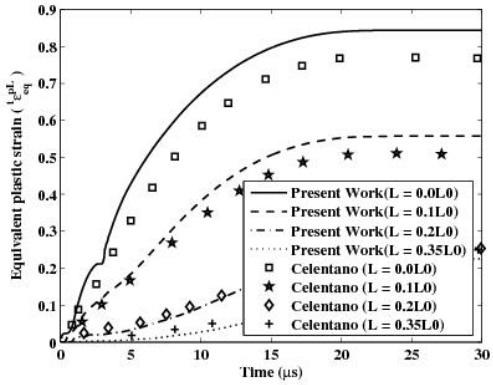

(d) Equivalent plastic strain on central axis

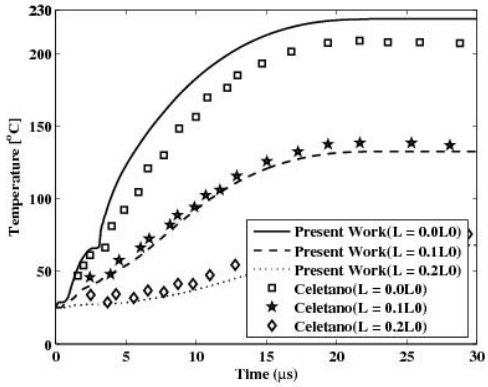

(e) Temperature on rod axis

Figure 2: Variation of computed characteristic parameters with time.

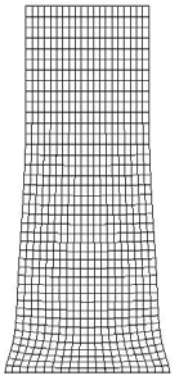

Figure 3: Deformed configuration.

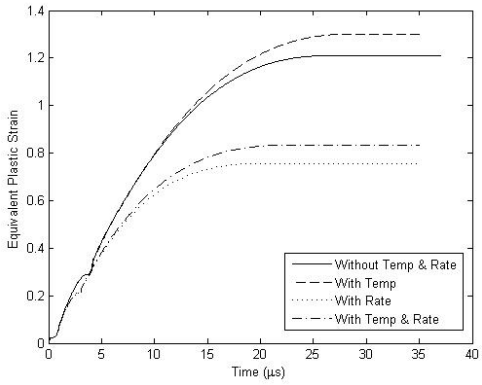

Figure 4: Effect of strain rate and temperature on equivalent plastic strain at the center of the impact face.

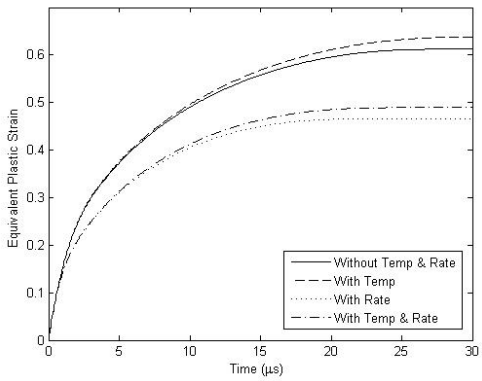

Figure 5: Effect of strain rate and temperature on equivalent plastic strain at the outer edge of the impact face.

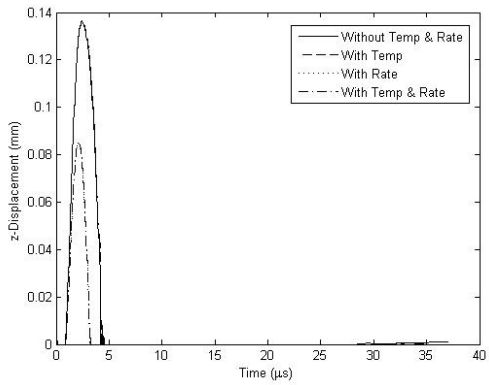

Figure 6: Variation in axial-displacement for the centre point on impact face with time.

The final length of the rod is denoted by L_f and the final radius of the impact face by R_f. Variations of L_f/L_0 and R_f/R_0 ratios with the impact velocity are presented in Figs. 2(a) - 2(b). The respective results from the reference are also presented. It is observed that the trends are in good agreement with experimental and numerical results of the Celentano (2002). The growths of equivalent plastic strain along the impact face at three points and along the central axis at few points at an impact velocity of 183 *m/s* is shown in Figs. 2(c) -2(d). These results are in good agreement with the numerical results of Celentano (2002). Further, the temperature rise at three points along the central axis for impact velocity of 183 *m/s* is shown in Fig. 2(e). These results are also in good agreement with the numerical results of Celentano (2002). Small deviation in the two sets of results is due to the selection of certain values for the Newmark's parameters used in the present formulation and the choice of factor β (i.e., the fraction of the plastic work getting converted into heat). This can be explained as follows:

1. In Celentano's work (2002), the integration of the terms containing the time derivatives of displacement (Eq. 18) is carried out with the Hilber-Hughes-Taylor (1977) method and the terms containing the time derivative of temperature (Eq. 24) is carried out using the generalized midpoint rule algorithm. In the present work, the integration of the terms containing the time derivatives of displacement (Eq. 15) is carried out using the Newmark's scheme (Bathe 1996). The integration of the terms containing the time derivative of temperature (Eq. 24) is carried out using the general finite difference scheme.
2. In Celentano's work (2002), the value of β is not mentioned. In the experimental work of Farren and Taylor (1925), the fraction of plastic work getting converted into heat is experimentally measured. For Steel, the fraction is 86.5%. In the numerical simulation of fracture in Taylor rod impact test by Teng *et al.* (2005), it is mentioned that this fraction is usually taken as 90%. Hence, in the present work, β is selected as 0.9.

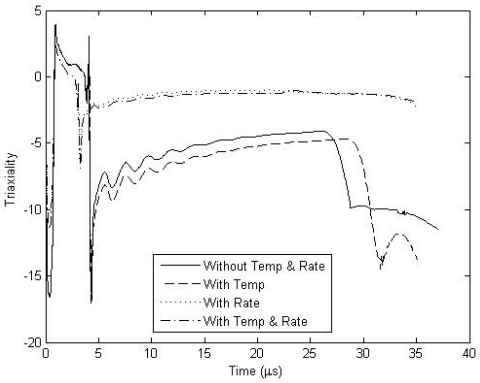

Figure 7: Effect of strain rate and temperature on triaxiality at the centre of the impact face

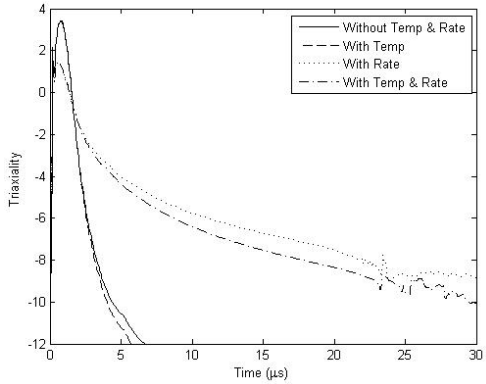

Figure 8: Effect of strain rate and temperature on triaxiality at the outer edge of the impact face

7.2. *Effect of strain rate and temperature*

Equivalent plastic strain and triaxiality are the continuum parameters which influence the fracture in ductile materials (Saxena and Dixit 2011). Next, the FEM code is employed for carrying out the study of the effects of strain rate and temperature on equivalent plastic strain and triaxiality in Taylor rod impact problem. The un-deformed geometry of the problem domain is shown in Fig. 1. The material properties for SAE 1020 steel are given in Table 1. The rod is impacted on a rigid wall at an impact velocity of 183 *m/s*. The deformed configuration of the Taylor rod is shown in Fig. 3.

Figures 4–5 show the growth of equivalent plastic strain at the center and at the edge of the impact face. The value of equivalent plastic strain increases at a very high rate and becomes constant within 12-15 μs. Further, it is observed that in all the cases the value of equivalent plastic strain becomes constant on the axis of the rod for a short duration at around 3-5 μs (Fig. 4). This is due to the fact that the material at the rod axis is not in contact with the rigid surface for this short duration of time (Fig. 6) resulting in unloading and the material becomes elastic. After a very short duration the material again comes into contact with the surface of the wall. Therefore, it starts deforming again and becomes plastic as is evident from Fig. 4. This phenomenon is not observed at the edge of the rod (Fig. 5) hence there is no unloading at the outer edge throughout the deformation. Figures 4-5 show that, initially the edge of the impact face has a higher value of equivalent plastic strain in comparison to the center point. This is because the outer surface of the rod at the impacted end moves at a very high velocity and initial plastic deformation is observed at the outer edge. Later, the plastic deformation advances towards the central axis of the rod material and its value becomes maximum at the centre.

It is observed from Figs. 4-5 that the value of equivalent plastic strain ${}^{t}\varepsilon_{eq}^{pL}$ is the largest if only the effect of temperature is considered as compared to the other cases. This is due to temperature softening of the material resulting into an increase in the plastic deformation. It is observed that the value of ${}^{t}\varepsilon_{eq}^{pL}$ is smallest, if the effect of strain rate is considered, neglecting the effect of temperature. The value of ${}^{t}\varepsilon_{eq}^{pL}$ with strain rate is smallest due to the hardening of rod material. Further, it is observed that the value of ${}^{t}\varepsilon_{eq}^{pL}$ increases by about 8% when the effect of temperature is considered in comparison to without strain rate and temperature. The value of ${}^{t}\varepsilon_{eq}^{pL}$ decreases by about 35% due to strain rate effect only, in comparison to without rate and temperature. Thus, the strain rate has a much larger effect on the growth of equivalent plastic strain than the temperature. It is observed from Figs. 4-5 that the value of fracture strain gets over-predicted if the strain rate effect is not included.

Figures 7-8 show the variation of triaxiality with time at the impact face. At the center, the triaxiality value fluctuates in the initial period for all the cases. The magnitude of triaxiality is observed to be small when the effects of strain rate or temperature and strain rate are included in comparison to without strain rate and temperature. Further it is observed that the magnitude and variation of triaxiality are not affected much if the effect of temperature is included excluding the effect of strain rate. Teng *et al.* (2005) observed that at high velocity the fracture initiates at the center of the impact face in ductile material. At the centre of the impact face the magnitude of triaxiality is small (Fig. 7) and the magnitude of equivalent plastic strain is large (Fig. 4). The fracture due to high velocity impact in ductile materials is dependent on equivalent plastic strain and

temperature (Lemaitre and Desmorat 2005), therefore, the fracture is likely to initiate at the centre of the impact face due to larger value of ${}^{t}\varepsilon_{eq}^{pL}$. This phenomenon is called as confined fracture (Teng *et al.* 2005).

8. Conclusions

A coupled thermo-elasto-plastic formulation is developed. The formulation is employed for the numerical study of the effects of strain rate and temperature on the equivalent plastic strain and triaxiality in the Taylor rod impact problem. The growth of equivalent plastic strain and temperature along the impact face and along the central axis of the rod are consistent with the results reported in literature. It is found that the strain rate has a larger effect on the growth of equivalent plastic strain and triaxiality than the temperature. The fracture strain is over-predicted if the strain rate effect is not included in the analysis. It is found that the strain rate has a prominent effect than the temperature on ensuing fracture in high velocity impacts. The presented work has been extended to impact fracture of Taylor rod and cylindrical tubes [Gautam and Dixit 2011a; 2011b].

References

Bathe, K. J., 1996, Finite element procedures. Prentice Hall of India, New Delhi.

Brünig, M. and Driemeier, L., 2007, Numerical simulation of the Taylor impact test. Int. J. Plast, vol. 23, pp. 1979–2003. (http://www.sciencedirect.com/science/article/pii/S0749641907000137)

Celentano, D. J., 2002, Thermo-mechanical analysis of the Taylor impact test. J. App. Phy., vol. 91, pp. 3675–3686. (http://jap.aip.org/resource/1/japiau/v91/i6/p3675_s1?isAuthorized=no)

Farren W. S. and Taylor T. I., 1925, The heat developed during plastic extension of metal. Proc. R. Soc. London A, vol. 107(743), pp. 422–451.

Gao, Y. and Wagoner, R. H., 1987, A simplified model of heat generation effects during the uniaxial tensile test. Metall. Trans. A, vol. 18A, pp. 1001–1009. (http://adsabs.harvard.edu/abs/1991MTA....22.1001G)

Gautam, S. S. and Dixit, P. M., 2011a, Ductile fracture simulation in the Taylor rod impact test using continuum damage mechanics, Int. J. Damage Mech., vol. 20, pp. 347-369. http://ijd.sagepub.com/content/early/2010/02/08/1056789509357119?patientinform-links=yes&legid=spijd;1056789509357119v1)

Gautam, S. S. and Dixit, P. M., 2011b, Numerical simulation of ductile fracture in cylindrical tube impacted against a rigid surface, Int. J. Damage Mech., doi: 10.1177/1056789511398883.
(http://ijd.sagepub.com/content/early/2011/04/22/1056789511398883.abstract)

Hilber, H. M., Hughes, T. J. R., and Taylor, R. L., 1977, Improved numerical dissipation for time integration algorithms in structural dynamics, Earthquake Eng. Struct. Dyn., 5, pp. 283–292. (http://onlinelibrary.wiley.com/doi/10.1002/eqe.4290050306)

Hodowany J., Ravichandran G., Rosakis A. J. and Rosakis P., 2000, Partition of plastic work into heat and stored energy in metals, Exp. Mechanics, vol. 40(2), pp. 113-123.

Hsu, T. R., 1986, The finite element methods in thermo-mechanics, Allen & Unwin, London.

Johnson, G. R. and Cook, W. H., 1985, Fracture characteristics of three metals subjected to various strains, strain rates and temperatures and pressures. Engg. Fract. Mech., vol. 1(1), pp. 31–48. (http://www.sciencedirect.com/science/article/pii/0013794485900529)

Kamlah M. and Haupt P., 1997, On the macroscopic description of stored energy and self heating during plastic deformation, Int. J. Plast., vol. 13(10), pp. 893-911.
(http://www.sciencedirect.com/science/article/pii/S0749641997000636)

Lemaitre, J. and Desmorat, R., 2005, Engineering damage mechanics, Springer-Verlag, Berlin, Heidelberg.

Mason, J. J., Rosakis, A. J., and Ravichandran, G., 1993, On the strain and strain-rate dependence of the fraction of plastic work converted into heat: an experimental study using high-speed infrared detectors and the Kolsky bar. Mech. Mater., vol. 17, pp. 135–145.

Mollica F., Rajagopal K. R. and Srinivasa A. R., 2001, The inelastic behavior of metals subject to loading reversal, Int. J. Plast., vol. 17, pp. 1119-1146. (http://www.sciencedirect.com/science/article/pii/S0749641900000826)

Saxena, R. K. and Dixit, P. M., 2011, Numerical analysis of damage for prediction of fracture initiation in deep drawing, Finite Elem in Anal Design, vol. 47(9), pp 1104-1117. (http://www.sciencedirect.com/science/article/pii/S0168874X11000850)

Taylor G.I and Quinney H., 1934, The latent energy remaining in a metal after cold working, Proc. R. Soc. Lond. A, vol.143, pp 307-326. (http://rspa.royalsocietypublishing.org/content/143/849/307)

Teng, X., Wierzbicki, T., Hiermaier, S., and Rohr, I., 2005, Numerical prediction of fracture in the Taylor test. Int. J. Solids Struct., vol. 42, pp. 2929–2948. (http://www.sciencedirect.com/science/article/pii/S0020768304005414)

Taylor, G., 1948, The use of flat-ended projectiles for determining dynamic yield stress, theoretical considerations. Proc. Roy. Soc. London A, vol. 94, pp. 289–299. (http://rspa.royalsocietypublishing.org/content/194/1038/289)

Varadhan, S. N., 1997, Dynamic large deformation elasto-plastic analysis of continua. Master's thesis, Department of Mechanical Engineering, IIT Kanpur.

Wriggers, P. and Miehe, C., 1994, Contact constraints within coupled thermo-mechanical analysis – A finite element model. Comput. Methods Appl. Mech. Engg., vol. 113, pp. 301–319. (http://www.sciencedirect.com/science/article/pii/0045782594900515)

Xing, H. L. and Makinouchi, A., 2002, FE modeling of thermo-elasto-plastic finite deformation and its application in sheet warm forming. Engg. Comput., vol. 19, pp. 392–410. (http://www.emeraldinsight.com/journals.htm?articleid=1455476)

Zhong, Z. H., 1993, Finite element procedures for contact-impact problems. Oxford University Press, Oxford.